Self-cleaning hybrid hydrophobic-hydrophilic surfaces: durability and effect of artificial soilant particle type

Illya Nayshevsky[1,2], QianFeng Xu[3], Jimmy M. Newkirk[4], Daniel Furhang[1],
David C. Miller[4], and Alan M. Lyons[1,2,3]

[1] College of Staten Island, City University of New York, 2800 Victory Blvd, Staten Island, NY 10314
[2] The Graduate Center, City University of New York, 365 5th Avenue, New York, NY 10016
[3] ARL Designs LLC, 215 W 125th Street 4th Fl., New York, NY 10027
[4] National Renewable Energy Laboratory (NREL), 15013 Denver West Pkwy, Golden, CO 80401

Abstract — **Dew accelerates soiling rates and increases dust adhesion. To use dew for self-cleaning, a fluorinated ethylene propylene (FEP) coating was applied to suppress reactions between dust and glass as well as facilitate dew to condense as mobile droplets. An array of rectangular hydrophilic channels in the coating increases condensation rates and droplet slide-off diameters. The durability of the coating was evaluated by artificial UV weathering. Four different types of soilants were used in artificial soiling tests to assess the effect of soilant type and surface properties on soiling rates and self-cleaning efficacy under simulated dew conditions. Soil deposition and self-cleaning mechanisms are be reported.**

Index Terms — **anti-soiling, hydrophilic, hydrophobic coating, self-cleaning, soiling**

I. INTRODUCTION

Soiling of photovoltaic (PV) cover glass is known to reduce the electrical output by 4-7 % in North America and Europe [1]–[8] and up to 70 % in other locations [4], [5], [8]–[11]. Natural condensation, or dew, has been shown to accelerate soiling rates [4], [5], [8], [12]–[14] and facilitate the adhesion of particulate matter on solar cover glass [4], [12], [14]. Because of the strong interactions between glass and water, dew will spread out, forming a liquid film on the glass. Soiling rates depend on environmental conditions as well as through surface interaction mechanisms, the chemical properties of the glass surface, as well as the chemical composition of the dust itself. Soluble compounds within the contaminant particles can chemically react with the liquid and glass interfaces causing crystallization and/or cementation reactions to occur as the dew evaporates glass [4], [12], [14] . As a result, such particles can become more strongly adhered to the surface [15]. In addition, surface reactions will affect the cleaning processes required to remove the soil. Strongly bound soil will require mechanical brushing with water [4], [9] to restore performance whereas weakly bound dust can be easily removed with water alone. Thus, there is a need for coatings that can impart both anti-soiling as well as self-cleaning properties to solar cover glass.

Anti-soiling properties increase the amount of energy that a PV panel can produce in a given environment, by reducing the optical losses resulting from soilant absorption and scattering.

Self-cleaning properties decrease mechanical cleaning frequency/duration and so reduce operation and maintenance (O&M) costs by using naturally occurring dew or precipitation to wash away particulates without using mechanical brushing.

Our group has shown that a hydrophobic coating on glass (water contact angle (CA) of $\geq$ 90°) reduces soiling rates compared to uncoated surfaces in the presence of condensed water [16]. Optical losses due to ISO 12103 A2 Arizona Test Dust deposition were reduced by 45 % on hydrophobic coatings compared to uncoated surfaces. The lower soiling rate results from a dust herding mechanism, where highly mobile liquid water droplets sweep dust particles into concentrated piles as the droplet's solid-liquid-vapor triple contact line (TCL) contracts during evaporation. We have also shown that water collection from simulated dew can be increased by more than 36 % by incorporating an array of hydrophilic features on the hydrophobic coating [17].

In this paper we examine the effect of surface coating and soil composition on soiling rates as well as cleaning efficacy using an enhanced, rectangular shape for the peripheral hydrophilic features. Hybrid hydrophobic-hydrophilic surface coatings were fabricated to optimize water collection rates under simulated dew conditions. Four types of soilants with different chemical properties (Arizona Test Dust, Aramco Test Dust, calcium carbonate and Portland cement) were studied to determine the effect of soilant solubility and reactivity on soiling rates. In addition, self-cleaning studies were conducted under simulated dew conditions to quantify the ability of dew to clean dust, as a function of dust composition. Coating durability was evaluated using artificial UV weathering tests.

II. METHODS

A. Material Fabrication

Three types of surfaces were studied: clean bare glass (Bare Glass), which is hydrophilic; glass with a hydrophobic polymer coating (Phobic); and glass with a hybrid hydrophobic-hydrophilic coating (Hybrid). Low-iron Diamant (Saint-Gobain S.A.) glass substrates, 3 mm thick and cut to 50 mm x 57 mm, were used for all experiments. Substrates were cleaned by

washing with an Alconox-water solution (Alconox Inc.), rinsed with DI water and dried with compressed air before use.

Hydrophobic coated glass substrates were prepared by applying a <1 μm thick, fluorinated ethylene propylene (FEP) coating onto the cleaned glass using a lamination-peeling process [18]. Teflon® FEP film (American Durafilm) was laminated to the glass substrate at ≥ 275 °C for ≥ 5 minutes and allowed to cool below the melt point of the resin (260 °C). Excess polymer was peeled from the surface leaving a nanometer-thick coating of FEP strongly adhered to the glass.

Hybrid hydrophobic-hydrophilic (Hybrid) surfaces, shown schematically in Fig. 1, were prepared by creating hydrophilic channels in a hydrophobic coated glass substrate, previously prepared as described in the preceding paragraph. The hydrophilic channels were created by selectively abrading away the hydrophobic coating, revealing the underlying hydrophilic glass substrate. Pumice powder (~5 % by weight) dispersed in water, was rubbed against the coating using a plastic rod (0.5 mm diameter) guided by rectangular openings in a 3-D printed stencil. The stencil was 3-D printed using polylactic acid (PLA) filament. The width and spacing between the rectangular hydrophilic channels were systematically varied in order to optimize water collection efficiency. Rectangular hydrophilic channels were found to exhibit 78 % greater condensation cleaning rates than hydrophilic rings [17], [19]. Optimal dimensions of the channels were determined to be 0.6 mm x 20 mm on 1.7 mm pitch based on a parametric study [19]. A single row of 23 channels, each measuring 20 ± 0.3 mm tall (Fig 1a), 0.6 ± 0.1 mm wide and spaced 1.1 ± 0.1 mm apart (Fig 1b) was found to be optimal and positioned along the top edge of the Hybrid substrates.

B. Experimental Methods

Dust was applied to the glass substrates using an accelerated soiling apparatus [16] shown schematically in Fig. 2. The apparatus was designed to replicate dust deposition conditions in the Arizona desert [6]; water was allowed to condense on the surface, mimicking natural dew, immediately before airborne dust deposition. After dust deposition, samples were baked before beginning the next deposition cycle. All samples were exposed to three dew-deposition-bake cycles.

A 20 mg sample of test dust was used per cycle. The test dusts used included: Standard Arizona Test Dust (A2 Fine Grade ISO 12103-1, PTI Inc.), Aramco Test Dust (PTI Inc.), calcium carbonate (particle diameter <50 μm, Sigma Aldrich) and Portland cement (PTI Inc). Humidity inside the chamber was stabilized (70 %RH) and samples were cooled to 10 °C for 2 minutes, using a Peltier device, to induce condensation on the surface. Dust was injected upwards into the dust tunnel by
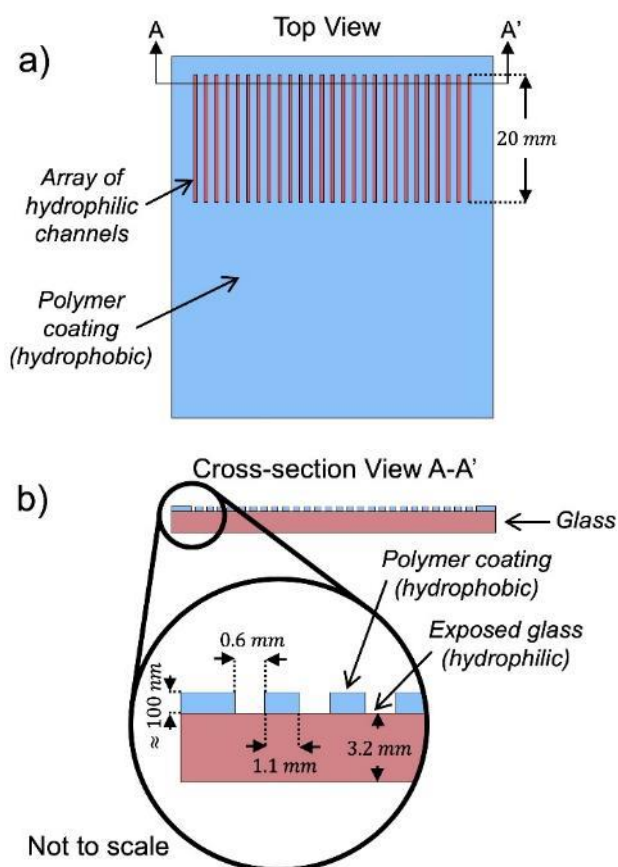

Fig. 1. Drawing of a hybrid surface showing a) top and b) cross-sectional views. The dimensioned schematic shows the hydrophobic polymer coating on a glass substrate with exposed glass hydrophilic channel array.
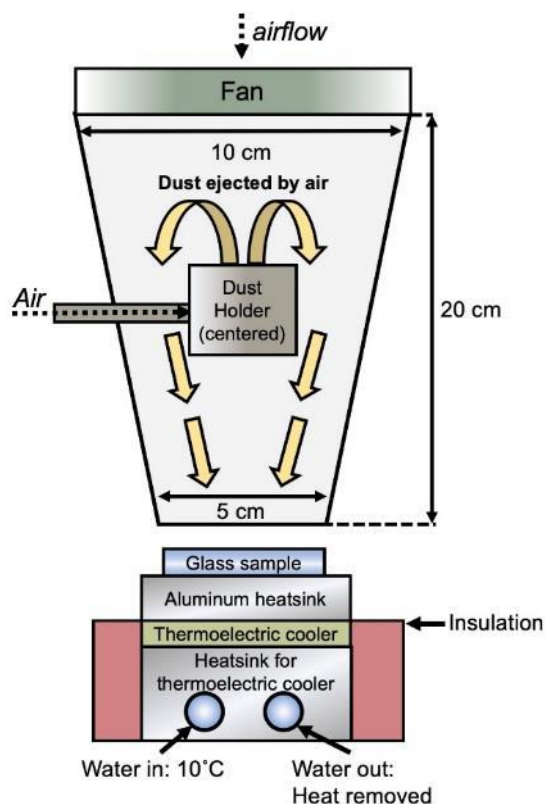

Fig. 2. Schematic of artificial soiling chamber.

applying a pulse of dry compressed air (20 psi, 30 secs). The overhead fan (3 m/s), dispersed the dust so that it covered the underlying glass. Lastly, the same thermoelectric Peltier device was used to heat the samples to 50 °C for 10 min to facilitate dew evaporation and enable cementation and/or recrystallization of minerals. The time between the deposition cycles was 10-15 minutes (the time required to obtain microscopy images and optical transmittance measurements).

A separate artificial dew chamber, shown schematically in Fig. 3, with samples positioned at one of the 3 tilt angles: 25°, 45° and 85° was used to study self-cleaning. Relative humidity in the chamber was maintained at ~90 % by evaporation from a saturated wick at room temperature. Samples were cooled to 10 °C, below the dew point of ~16 °C. Condensation rates and patterns were analyzed via a high definition camera controlled by a computer vision enabled Python programming language algorithm [20]. Condensation time for each set of samples (1x Bare Glass, 2x Phobic and 1x Hybrid coupon per experiment) was determined by the amount of time required for water droplets to slide off from a complete row of hydrophilic channels on the Hybrid surface.
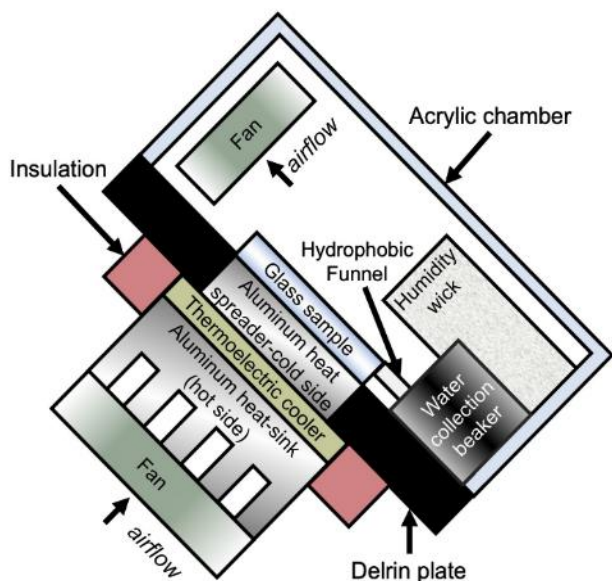

Fig. 3.   Schematic of artificial dew cleaning chamber.

C. Analytical Methods and Automation Controls.

For anti-soiling and self-cleaning experiments, soiling was quantified by direct optical transmittance (%τ) at a wavelength (λ) of 550 nm. Transmittance was recorded using a Lambda 650 UV-VIS spectrophotometer (PerkinElmer Inc.). Three separate 0.6 cm2 (0.4 cm x 1.5 cm) areas were measured on each sample, the average of the three results is reported. A single wavelength direct transmittance measurement was used, as opposed to the representative solar-weighted transmittance as per IEC 62788-1-4 [21], [22] for rapid quantification of optical performance.

Several considerations should be remembered regarding assessment at a single optical wavelength. It is well-known that particles scatter shorter wavelengths of light more efficiently than longer wavelengths [23]. This is especially true since most of the soil particles that are found on solar modules are less than 16 microns in diameter [24]. Using field data, Qasem showed [25] that wavelengths below 570 nm are the most sensitive to soiling. The disproportionate impact of soil particulates on shorter wavelengths (<600 nm) was also recently reported by Tanesab [26]. However, there is a lower limit to the optimal wavelength that can be used. Due to the lesser energy present at $\lambda < 400$ nm in the global terrestrial solar spectrum AM1.5 [27] and the spectral response of most semiconductors used for PV, wavelengths above 500 nm are of greatest relevance to characterize PV module soiling. Micheli et al. recently correlated soiling losses to transmittance measurements comparing results from a single wavelength to different spectral ranges [28]. The correlation between singlet wavelength hemispherical transmittance measurements at 550 nm and the Soiling Ratio (as defined by IEC 61724-1)[29] was greater than 98 % for all PV material absorbers. They concluded that soiling can be estimated by using the transmittance at a single wavelength with high accuracy. Moreover, a single wavelength measurement is more economical, and direct transmittance is more sensitive to soiling and more widely available than hemispherical transmittance measurements. This is especially true when analyzing a large number of samples with redundant measurements. As a result of these considerations, a wavelength of 550 nm was used for direct transmittance measurements for all soiling and cleaning experiments.

Surface coverage of dust and soiling trends were observed via digital optical microscopy (Nikon SMZ 1500 using INFINITY2-1C camera). Water contact angles (CA) were measured using a model 250-F1 contact angle goniometer (ramé-hart Instrument Co.) Ten measurements per coupon were automatically performed using 5 µL droplets of DI.

Indoor accelerated weathering tests were conducted using a Ci5000 Xenon Weather-ometer test chamber (Atlas Material Testing Technology LLC) following the IEC TS 62788-7-2 A3 method [30], i.e., irradiance of 0.8 W·m-2·nm-1 at 340 nm, chamber temperature of 65 °C, black panel temperature of 90 °C, and chamber relative humidity of 20 %. Solar grade Acrylite 0Z023 GT poly(methyl methacrylate) sheet ("Acrylic", Evonik Industries AG), 3.2 mm thick, was used as a reference material. Direct optical transmittance of the accelerated weathering test samples were measured from 200 nm to 2500 nm using a Cary 5000 dual-beam ultraviolet-visible-near infrared (UV-VIS-NIR) spectrophotometer (Agilent Technologies Inc.) Contact angle values during Weather-ometer testing were measured with a "100–25–A" goniometer (ramé-hart Instrument Co.) Ten measurements were automatically performed using 4 µL of deionized water at three different locations within the same coupon, providing an average result for 30 measurements.

III. RESULTS

A. Optical and Wetting Properties

As prepared, the Bare Glass samples (12 replicates) exhibit a direct transmittance at 550 nm (%τ) of 91.8 ± 0.1 % and are hydrophilic (CA = 9.1 ± 1.5°). In contrast, the Phobic (24 replicates) and Hybrid (8 replicates) samples are more transparent because the fluoropolymer coating imparts anti-reflectivity (%τ = 93.6 ± 0.6 % and 94.0 ± 0.2 % respectively). These coated surfaces are hydrophobic, with contact angle values of 119 ± 2°.

B. Artificial Weathering

The optical and surface properties of the Phobic glass are stable when exposed to artificial weathering. As shown in Fig. 4a, the direct representative solar weighted transmittance (RSWT) evaluated from 300 nm − 1250 nm [21], [22] remains stable after 7.2 MJ·m$_{-2}$ (2000 h) of cumulative radiant exposure. Moreover, the surface energy of the Phobic coating remains unchanged as the water CA remained above 117° (Fig. 4b). These results indicate that the surface chemistry of the fluoropolymer coating remains intact through the weathering shown in Fig. 4.
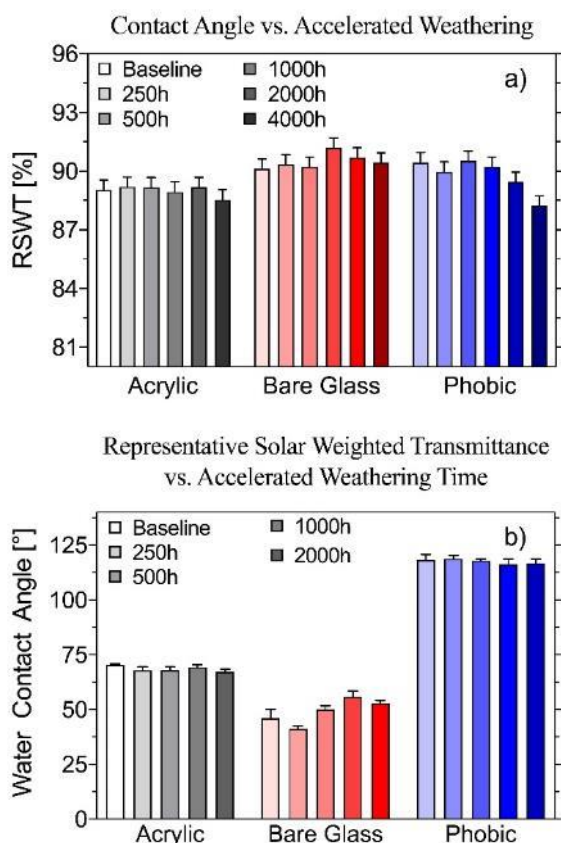

Fig. 4. Properties of control and coated Phobic substrates subjected to 2000 h of accelerated indoor weathering: a) change in solar weighted direct transmittance; b) change in CA.
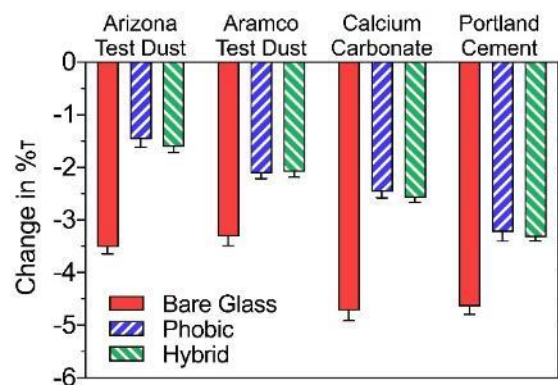

Fig. 5. Change in %τ at 550 nm as a function of soilant type and surface coating for Bare Glass, Phobic and Hybrid coatings after three dew-dust-bake soil deposition cycles; averaged over $n = 3$ soiling trials.

C. Anti-Soiling Properties

The performance loss from soiling depends strongly on the chemistry of both the glass surface coating as, well as the type of soilant. The total change in %τ after three dew-dust-bake cycles for each dust type and surface coating is shown in Fig. 5. Soiling loss was observed to be higher on Bare Glass than on Phobic or Hybrid glass surfaces for all soil types. Combining data for all soil types, the average decrease in %τ at λ = 550 nm on Bare Glass is 4.1 ± 0.3 % (1.5 ± 0.3 % per dust application), whereas on Phobic and Hybrid surfaces the overall change was 2.3 ± 0.3 % and 2.4 ± 0.2 %, respectively. Phobic and Hybrid surfaces exhibit anti-soiling behavior compared to Bare Glass for all four types of soilants tested; these hydrophobic coatings outperform Bare Glass by 41.7 ± 6.8 %. Hybrid and Phobic samples exhibit the same soiling deposition as expected, because the hydrophobic surface coatings are prepared using the same method.

Soiling on all surface types are lower for soils that do not react with water (Arizona Test Dust) and/or contain NaCl (Aramco Test Dust), which is highly soluble in water. In contrast, calcium carbonate ($CaCO_3$) and Portland cement, which can react with water [31], [32], soil at higher rates than

TABLE I
SOILANT TYPE, COMPOSITION, SOLUBILITY, AND CHANGE IN
OPTICAL PERFORMANCE

Soilant	Relevant Chemical Compound	Solubility in water	Soiling on Bare Glass, Δ%τ	Soiling on Phobic + Hybrid, Δ%τ
AZ Dust	Silicates	Negligible	-3.5 ± 0.1 %	-1.5 ± 0.1%
Aramco	10% NaCl	360 g/L	-3.3 ± 0.2 %	-2.1 ± 0.1%
Calcite	$CaCO_3$	0.047 g/L	-4.7 ± 0.2 %	-2.5 ± 0.1%
Cement	CaO	Negligible	-4.6 ± 0.2 %	-3.3 ± 0.1%

▣ Reactive compounds

the silicate-based soils (Table 1). $CaCO_3$ is soluble in water at pH 5.7 (the pH of water saturated with atmospheric CO_2). Upon dissolution, calcium carbonate reacts with water to form CO_2 and $Ca(OH)_2$, the latter can further react with glass. The CaO in cement reacts exothermically with water also forming $Ca(OH)_2$. The greater soiling losses for the two water-reactive compounds are observed on all surface types but are most apparent on Bare Glass, as shown in Fig 5. Of the four soils studied, Portland cement results in the greatest soiling losses.

Anti-soiling effectiveness can also be compared qualitatively by visual comparison of Bare Glass, Phobic and Hybrid surfaces after 3 dew-dust-bake cycles (Fig. 6). The amount of soil deposited on Bare Glass (Fig. 6a) is qualitatively seen to be greater compared to Phobic and Hybrid surfaces (Fig. 6b, 6c) supporting the spectroscopic results. Phobic and Hybrid surfaces soil to a lesser degree, due to the "dust herding" mechanism previously reported [16].

D. Self-Cleaning Properties

Self-cleaning of the artificial soil was observed in the condensation chamber where liquid water condenses from the vapor phase (90 % RH at 25 °C) into liquid on the glass surfaces cooled to 10 °C, simulating natural dew. The percent of the original optical transmittance (%τ) restored after cleaning in the condensation chamber for all samples studied, including the four soil types and three tilt angles, are presented in Fig. 7. For Bare Glass samples, water condenses in a film-wise manner. Dust particles become suspended within the liquid water film and are redistributed during drying, resulting in additional scattering of light. The %τ decreases from between 0.1 % and 3.5 % (average 1.8 ± 1.7 %) after condensation, averaged over all soil types. The relatively large variance of %τ values measured on Bare Glass after condensation cleaning (Fig. 7) is caused by the heterogeneous redistribution of soil on the surface. Regions where water slides off the surface are relatively clean (Fig. 6 d), but because much of the liquid water condensed on the surface does not slide off, large dust spots form on most Bare Glass samples during the drying step as
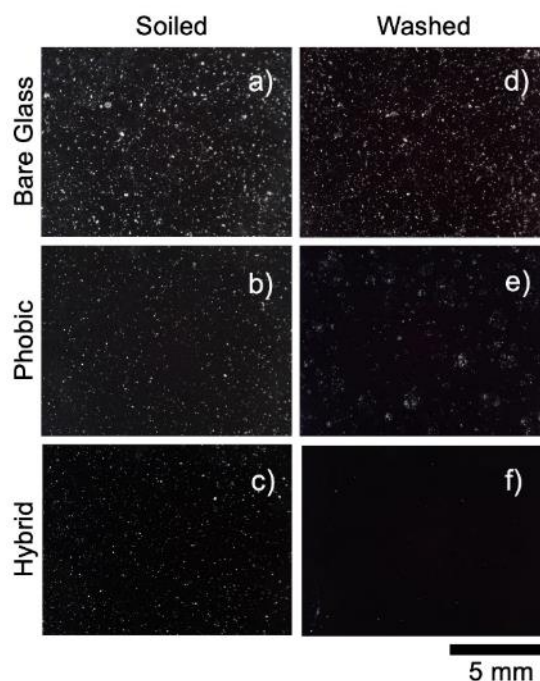

Fig. 6. Optical microscopy images of Bare Glass, Phobic and Hybrid surfaces after 3 dew-dust-bake cycles (a, b, c, respectively) and after simulated dew cleaning at 45° tilt angle (d, e, f, respectively), soiled with Portland cement test dust.

shown in Fig. 8. This leaves randomly arrayed cleaned and soiled regions that are comparable in size to the light beam emitted by the spectrophotometer (0.4 cm x 1.5 cm).

In contrast, on Phobic and Hybrid surfaces, water droplets nucleate, grow and slide-off, thereby carrying away soil particles, resulting in increased %τ values. Therefore, Phobic and Hybrid surfaces are cleaned efficiently by condensation; %τ increases by 1.3 ± 1.1 % and 1.6 ± 1.1 % respectively after
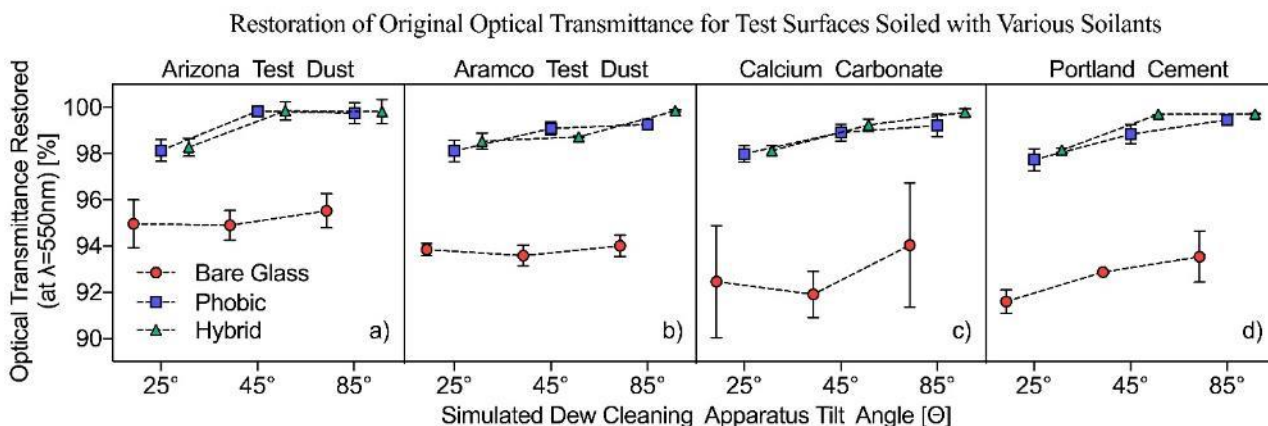

Fig. 7. Restoration of original %τ as a function of simulated dew cleaning tilt angle on Bare Glass, hydrophobic (Phobic) and Hybrid coatings after three dew-deposit-bake soil deposition cycles; utilizing a) Arizona Test Dust, b) Aramco Test Dust, c) Calcium Carbonate, and d) Portland Cement.
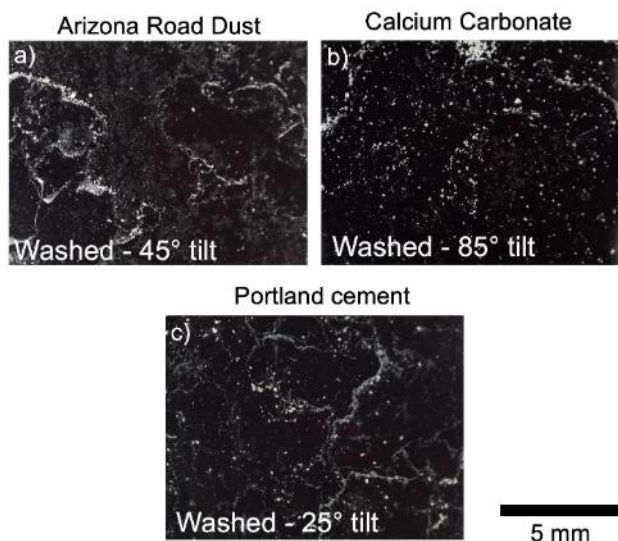
Fig. 8. Optical microscopy images of Bare Glass, soiled with a) Arizona Test Dust, b) Calcium Carbonate and c) Portland cement followed by condensation cleaning step at 45°, 85°, and 25° tilt angles respectively. The images show heterogeneous redistribution of soil after condensation cleaning on the surface of the glass.

~1 hour, recovering to 98.7 ± 0.3 % and 99.2 ± 0.1 % of the original %τ (Fig. 7), averaged over all soil types and tilt angles.

The angle of substrates positioned within the condensation chamber affects the efficiency with which artificial dew can clean the surfaces. Substrates at higher tilt angles are cleaned more effectively for all types of coatings as well as all soil types, as shown in Fig. 7. The largest improvement (1.2 %τ) is seen between a tilt angle of 25° and 45°. A smaller but still significant improvement is observed upon increasing the tilt angle to 85°.

Overall, Hybrid surfaces are cleaned more effectively than Phobic surfaces, which are lacking hydrophilic channels. On the Hybrid surfaces, liquid water droplets are preferentially nucleated on the hydrophilic channels located along the top (up-slope) portion of the glass. The liquid water accumulates at the bottom of the channel until it reaches a critical mass then slides off the surface as shown in Fig. 9.

At any given tilt angle, droplets grow to a larger diameter on Hybrid surfaces than on Phobic surfaces before sliding off the surface. For example, at 45°, the diameter of drops sliding off from a soiled Phobic surface measure 2.8 ± 0.8 mm, compared to 3.4 ± 1.0 mm on Hybrid surface. Because of the larger diameter, drops on a Hybrid surfaces clean away dust from a larger swath of the surface.

The difference in drop diameter measured at 25° tilt angle was more pronounced than at a 45° tilt angle with 3.0 ± 1.2 mm on Phobic surfaces and 5.5 ± 1.3 mm on Hybrid surfaces. The larger drop diameter on Hybrid surfaces is attributed to the strong water-glass interactions leading to water drop pinning on the hydrophilic regions of the hybrid surfaces. The lower tilt angle results in a smaller gravitational force component, thus increasing the water drop mass required to overcome the pinning forces at the glass-water-vapor triple contact line. In contrast, the drop diameters at an 85° tilt angle are 2.5 ± 0.5 mm on Phobic surface and 3.0 ± 0.5 mm on Hybrid surfaces. Optimization of the size of the hydrophilic features may improve performance at each tilt angle.

Hybrid surfaces result in improved cleaning effectiveness in a second important way, less time is required for a full row of liquid water drops to slide off from a complete row of hydrophilic channels on the Hybrid surface than a Phobic surface. Drops roll off 6.5 minutes faster from a Hybrid surface than from a Phobic surface (both at 45° tilt angle) for reactive soilants ($CaCO_3$ and Portland cement). This enables a Hybrid glass surface to be cleaned faster, thus using the limited naturally occurring dew more efficiently.

Visual comparison of surfaces cleaned with simulated dew confirm the spectrophotometer measurements and show that Phobic and Hybrid surfaces (Figs. 6e, 6f) were more effectively cleaned whereas the Bare Glass surface (Fig. 6d) was cleaned to a lesser degree. Portland cement is absent on the Hybrid surface in these images after condensation cleaning.
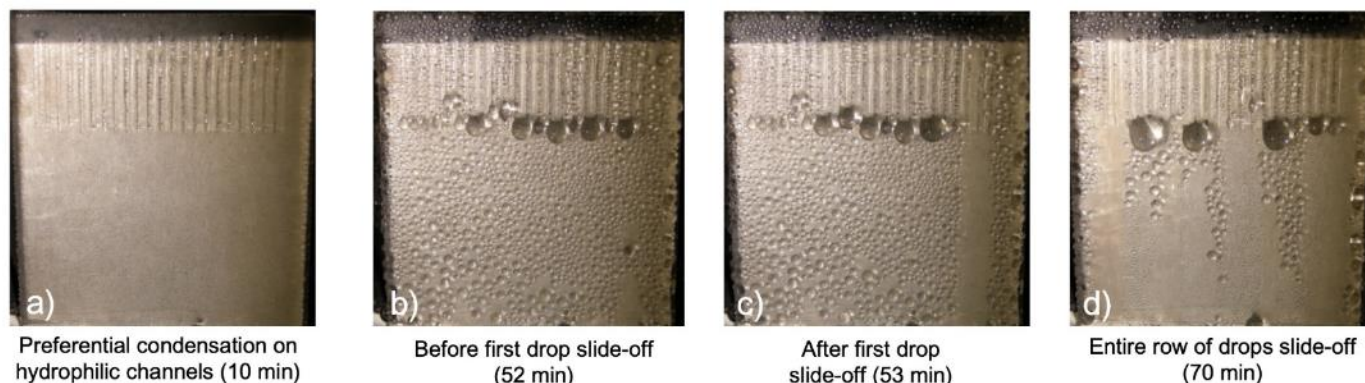

Fig. 9. Optical photographs of water condensing on a soiled Hybrid surface in the condensation chamber at 45° tilt angle and using Arizona Test Dust, a) water preferentially nucleates and grows on hydrophilic channels, b) liquid water drops accumulate at base of channels, c) initial drop slides off down the hydrophobic coated glass after reaching critical size (53 min); d) entire row of drops have slid off surface with new drops forming (70 mins).

IV. Conclusion

Hybrid surfaces comprised of a hydrophobic coating and hydrophilic channels positioned along the top (up-slope) edge of the glass provide both anti-soiling properties as well as self-cleaning behavior when placed in a condensing (simulated dew) environment. The anti-soiling properties are due primarily to the high water droplet mobility and chemical inertness of the fluoropolymer coating, which exhibits good durability, maintains high transparency (>90 % RSWT) and droplet mobility (CA >117°) after 2000 hours of accelerated weathering time. The chemically unreactive surface deters cementation and promotes a previously observed "dust herding" mechanism [16], [33] which concentrates dust into small, discrete piles. This minimizes the reduction in %τ after dew-dust-bake soiling cycles. Hybrid and Phobic surfaces exhibit the same anti-soiling properties; both reduce soiling by ~46 % compared to Bare Glass. Soils that can chemically react with water, such as calcium carbonate and Portland cement, were observed to soil at a faster rate on all surface types than silicate-based soils (Arizona Test Dust and Aramco Test Dust). The greater soiling accumulation with reactive soils are more pronounced on Bare Glass substrates than hydrophobic surfaces.

Hybrid and Phobic surfaces that have been artificially soiled exhibit self-cleaning behavior in the condensation chamber. The %τ at 550 nm of Hybrid and Phobic surfaces is restored to 99.2 % and 98.7 %, of their original transmittance values, respectively. In contrast, Bare Glass surfaces are not cleaned during artificial condensation. The %τ of the artificially soiled Bare Glass surfaces exhibit no significant change after the same time (~60 minutes) in the condensation chamber for all soil types. The low surface energy fluoropolymer coating prevents cementation reactions with the various soilants, facilitating the ability of liquid water droplets to carry soil away from the surfaces. On Bare Glass, stronger interactions between soil and glass, as well as water and glass, makes soil removal more difficult without the assistance of contact cleaning (risking abrasion). Hydrophilic channels increase cleaning efficacy because liquid water nucleates and grows more rapidly on a hydrophilic surface than a hydrophobic surface. As a result, droplets slide-off the channels approximately 10 % more rapidly than on a uniform hydrophobic surface. Moreover, the drops sliding off a Hybrid surface are larger in diameter than a Phobic surface, thereby cleaning a wider swath. The rectangular channel shape enables water to condense more efficiently as compared to the circular ring structures reported previously [16]. Higher tilt angles increase self-cleaning effectiveness for both Hybrid and Phobic surfaces.

Fabrication of full-size solar PV panels with hybrid coatings would be relatively straightforward to implement. A hydrophobic coating would be applied to the entire exterior-facing surface of the solar cover glass. Hydrophilic channels would be defined along the perimeter of the glass using the clearance and creepage regions to avoid the potential of these channels from adversely affecting light transmittance to the underlying semiconductors. Limiting the location of hydrophilic channels to this region would also enable the use of hydrophilic TiO_2 channels without affecting the reflection or absorption of light. Channels located only along the perimeter are anticipated to be sufficient for self-cleaning of full-sized modules because of the high mobility of water droplets on the hydrophobic coating. Once a single drop is released from a hydrophilic channel, the drop can slide down the entire length of the glass surface, cleaning a swath at least as wide as the drop along the entire length, or width, of the panel. Field experiments on glass substrates to validate these laboratory soiling and condensation test results are presently underway. Fabrication of functioning silicon modules is planned so that Soiling Ratio can be measured and the ability of droplets to traverse the entire panel can be validated.

References

[1]   J. Cano, "Photovoltaic Modules: Effect of Tilt Angle on Soiling," M.S. Dissertation, Arizona State University, 2011.

[2]   J. R. Caron and B. Littmann, "Direct monitoring of energy lost due to soiling on first solar modules in California," *IEEE J. Photovoltaics*, vol. 3, no. 1, pp. 336–340, 2013.

[3]   F. A. Mejia and J. Kleissl, "Soiling losses for solar photovoltaic systems in California," *Sol. Energy*, vol. 95, pp. 357–363, 2013.

[4]   T. Sarver, A. Al-Qaraghuli, and L. L. Kazmerski, "A comprehensive review of the impact of dust on the use of solar energy: History, investigations, results, literature, and mitigation approaches," *Renew. Sustain. Energy Rev.*, vol. 22, pp. 698–733, 2013.

[5]   A. Sayyah, M. N. Horenstein, and M. K. Mazumder, "Energy yield loss caused by dust deposition on photovoltaic panels," *Sol. Energy*, vol. 107, pp. 576–604, 2014.

[6]   W. Herrmann, M. Schweiger, G. Tamizhmani, B. Shisler, and C. Kamalaksha, "Soiling and self-cleaning of PV modules under the weather conditions of two locations in Arizona and South-East India," *2015 IEEE 42nd Photovolt. Spec. Conf. PVSC 2015*, pp. 1–5, 2015.

[7]   W. Herrmann, "Time evolution of PV soiling loss at test locations in different climates," in *Workshop „Soiling effect on PV modules"*, 2016, [Online] Available: https://www.tuv.com/media/corporate/solar_1/WHerrmann_Time-evolution-Soiling_Final.pdf

[8]   K. K. Ilse, B. W. Figgis, V. Naumann, C. Hagendorf, and J. Bagdahn, "Fundamentals of soiling processes on

photovoltaic modules," *Renew. Sustain. Energy Rev.*, vol. 98, no. September, pp. 239–254, 2018.

[9] S. Ghazi, A. Sayigh, and K. Ip, "Dust effect on flat surfaces - A review paper," *Renew. Sustain. Energy Rev.*, vol. 33, pp. 742–751, 2014.

[10] A. H. Hassan, U. A. Rahoma, H. K. Elminir, and A. M. Fathy, "Effect of airborne dust concentration on the performance of PV modules," *J. Astron. Soc. Egypt*, vol. 13, no. 1, pp. 24–38, 2005.

[11] A. Sayyah, M. N. Horenstein, and M. K. Mazumder, "Mitigation of soiling losses in concentrating solar collectors," *Conf. Rec. IEEE Photovolt. Spec. Conf.*, no. c, pp. 480–485, 2013.

[12] K. Ilse, M. Werner, V. Naumann, B. W. Figgis, C. Hagendorf, and J. Bagdahn, "Microstructural analysis of the cementation process during soiling on glass surfaces in arid and semi-arid climates," *Phys. Status Solidi - Rapid Res. Lett.*, vol. 10, no. 7, pp. 525–529, 2016.

[13] K. Ilse, B. Figgis, M. Z. Khan, V. Naumann, and C. Hagendorf, "Dew as a Detrimental Influencing Factor for Soiling of PV Modules," *IEEE J. Photovoltaics*, pp. 1–8, 2018.

[14] L. L. Kazmerski *et al.*, "Fundamental Studies of Adhesion of Dust to PV Module Surfaces: Chemical and Physical Relationships at the Microscale," *IEEE J. Photovoltaics*, vol. 6, no. 3, pp. 719–729, 2016.

[15] H. R. Moutinho *et al.*, "Adhesion mechanisms on solar glass: Effects of relative humidity, surface roughness, and particle shape and size," *Sol. Energy Mater. Sol. Cells*, vol. 172, no. July, pp. 145–153, 2017.

[16] I. Nayshevsky, Q. F. Xu, G. Barahman, and A. M. Lyons, "Fluoropolymer Coatings for Solar Cover Glass: Anti-Soiling Mechanisms in the Presence of Dew," *Sol. Energy Mater. Sol. Cells*. Accepted for publication (Nov. 4, 2019)

[17] I. Nayshevsky, Q. Xu, and A. M. Lyons, "Hydrophobic-Hydrophilic Surfaces Exhibiting Dropwise Condensation for Anti-Soiling Applications," *IEEE J. Photovoltaics*, vol. 9, no. 1, pp. 302–307, 2019.

[18] A. M. Lyons and Q. Xu, "Center-side method of producing superhydrophobic surface," US 9,987,818 B2, 2018.

[19] Q. Xu, I. Nayshevsky, D. Furhang, J. Newkirk, D. Miller, and A. M. Lyons, "A Hybrid Hydrophobic-Hydrophilic Coating with Anti-Reflective and Anti-Soiling Properties," in *Proceedings of the NREL PV Reliability Workshop*, 2019.

[20] I. Nayshevsky, "pyCondrop: Surface self-cleaning analytics." GitHub Repository: https://github.com/illyanayshevsky/pyCondrop.git, New York, NY, 2019.

[21] D. C. Miller *et al.*, "Examination of an Optical Transmittance Test for Photovoltaic Encapsulation Materials: Preprint NREL/CP-5200-60029," *SPIE Optics &*

Photonics, 2013. [Online]. Available: http://nrel-primo.hosted.exlibrisgroup.com/Pubs:PUBS:NREL_PUBS1 4c54c0f-e8d4-e411-b769-d89d67132a6d.

[22] *Measurement procedures for materials used in photovoltaic modules - Part 1-4: Encapsulants - Measurement of optical transmittance and calculation of the solar-weighted photon transmittance, yellowness index, and UV cut-off wavelength.* IEC 62788-4-1, International Electrochemical Commission, [Online] Available: https://webstore.iec.ch/publication/25942, 2016.

[23] D. J. Lockwood, *Rayleigh and Mie Scattering*. Springer, New York, NY, 2016.

[24] I. Nayshevsky, Q. Xu, and A. Lyons, "Literature Survey of Dust Particle Dimensions on Soiled Solar Panel Modules," in *2018 International PV Soiling Workshop*, 2018.

[25] H. Qasem, T. R. Betts, H. Müllejans, H. AlBusairi, and R. Gottschalg, "Dust-induced shading on photovoltaic modules," *Prog. Photovoltaics Res. Appl.*, vol. 22, pp. 218–226, 2014.

[26] J. Tanesab, D. Parlevliet, J. Whale, and T. Urmee, "The effect of dust with different morphologies on the performance degradation of photovoltaic modules," *Sustain. Energy Technol. Assessments*, vol. 31, pp. 347–354, 2019.

[27] *Photovoltaic devices - Part 3: Measurement principles for terrestrial photovoltaic (PV) solar devices with reference spectral irradiance data.* IEC 60904-3, International Electrochemical Commission, [Online] Available: https://webstore.iec.ch/publication/61084, 2008.

[28] L. Micheli *et al.*, "Correlating photovoltaic soiling losses to waveband and single-value transmittance measurements," *Energy*, vol. 180, pp. 376–386, 2019.

[29] *Photovoltaic system performance - Part 1: Monitoring.* IEC 61724-1:2017, International Electrochemical Commission, [Online] Available: https://webstore.iec.ch/publication/33622, 2017.

[30] *Measurement procedures for materials used in photovoltaic modules - Part 7-2: Environmental exposures - Accelerated weathering tests of polymeric materials.* IEC TS 62788-7-2, International Electrochemical Commission, [Online] Available: https://webstore.iec.ch/publication/33675, 2017.

[31] M.-A. Simard and C. Jolicoeur, "Chemical admixture-cement interactions: Phenomenology and physico-chemical concepts," *Cem. Concr. Compos.*, vol. 20, no. 2–3, pp. 87–101, 1998.

[32] F. Wolfgang Tegethoff, Ed., *Calcium Carbonate: From the Cretaceous Period into the 21st Century*. Birkhäuser Basel, 2001.

[33] K. K. Ilse *et al.*, "Comparing indoor and outdoor soiling experiments for different glass coatings and microstructural analysis of particle caking processes," *IEEE J. Photovoltaics*, vol. 8, no. 1, pp. 203–209, 2018.